Carbohydrate Polymers 89 (2012) 453–460

Contents lists available at SciVerse ScienceDirect

Carbohydrate Polymers

journal homepage: www.elsevier.com/locate/carbpol

In vitro evaluation of mucoadhesion and permeation enhancement of polymeric amphiphilic nanoparticles

Ya Liu[a], Hui Di Zang[a], Ming Kong[a], Fang Kui Ma[a], Qi Feng Dang[a], Xiao Jie Cheng[a,*], Qiu Xia Ji[b], Xi Guang Chen[a,*]

[a] College of Marine Life Science, Ocean University of China, Qingdao 266003, PR China
[b] The Affiliated Hospital of Medical College, Qingdao University, Qingdao 266001, PR China

ARTICLE INFO

Article history:
Received 6 January 2012
Received in revised form 22 February 2012
Accepted 8 March 2012
Available online 19 March 2012

Keywords:
OCMCS nanoparticles
Mucoadhesion
Permeation enhancement
In vitro Caco-2 cell model
Ex vivo carp intestines model

ABSTRACT

Oleoyl-carboxymethy-chitosan (OCMCS) nanoparticles based on chitosan with various molecular weights were prepared using coacervation process, which demonstrated particle size of 150–350 nm, zeta potential of 10–20 mV, and high encapsulation efficiency of fluorescein isothiocyanate dextran (FD4). OCMCS nanoparticles were found to be adsorbed onto the excised carp intestinal mucosa, the extent of adsorption increased with increasing chitosan molecular weight. In comparison to FD4 solution, OCMCS nanoparticles promoted FD4 transport through excised carp intestinal mucosa by 3.26–6.52 folds, which were observed via fluorescence microscope. The OCMCS nanoparticulate systems that interacted with the Caco-2 cells decreased the transepithelial electric resistance (TEER) and induced increasing the apparent permeability coefficient (P_{app}) of FD4 by 3.61–6.32 folds. Cytotoxicity studies in Caco-2 monolayers verified the safety of the delivery system. The improvement of mucoadhesive ability and permeability enable the OCMCS nanosystems suitable carriers for the intestinal absorption of protein drugs.

1. Introduction

The oral route offers a convenient alternative for the needle-free systemic delivery of protein drugs. Unfortunately, the intestinal absorption of these drugs is challenged by their poor membrane permeability as a result of high molecular weight, hydrophilicity, and surface charge (Yin, Chen, Qiao, Lu, & Hu, 2006). Mucoadhesive drug delivery systems exploit the attraction between polymers used in drug formulations and the mucus layer that covers epithelial surfaces throughout the body, including the gastrointestinal (GI) tract (Jinno, Oh, Crison, & Amidon, 2000; Peppas, Bures, Leobandung, & Ichikawa, 2000). Adhesion of a delivery system to the mucus layer provides localization within a specific body site and prolongs residence time, thus it greatly enhances the bioavailability of drugs, especially peptides and proteins (Chowdary & Srinivasa Rao, 2004).

Nanoparticles are well known to transport and deliver drugs which are unstable in the biological fluids and cannot readily diffuse across the mucosal barrier (Porporatto, Bianco, & Correa, 2005). Various approaches were applied to prepare nanoparticles, among which coacervation between oppositely charged polymers and drugs without use of organic solvent or sonication became a preferable alternative (Mao, Bakowsky, Jintapattanakit, & Kissel, 2006) Properties of the nanoparticles were largely dependent on the polymer employed. Therefore, nanoparticles containing polymeric enhancers or mucoadhesive polymers would be advantageous for oral delivery of protein drugs (Pinto, Neufeld, Ribeiro, & Veiga, 2006). They can transit directly and/or adhere to the mucosa, which is a prerequisite before the translocation process of particles (Dudhani & Kosaraju, 2010).

Chitosan is a biodegradable, biocompatible, and nontoxic polysaccharide that can adhere to the mucous layer by establishment of electrostatic interactions with sialic groups of mucin (Janes, Calvo, & Alonso, 2001). Moreover, chitosan has been shown to be a potential penetration enhancer (Mohammadia et al., 2011), which facilitated opening of the epithelial tight junctions (Yamamoto, Kuno, Sugimoto, Takeuchi, & Kawashima, 2005a; Yamamoto, Kuno, Sugimoto, Takeuchi, & Kawashima, 2005b; van der Lubben, Verhoef, van Aelst, Borchard, & Junginger, 2001). Chitosan is thereby able to enhance the paracellular route of absorption, which is important for the transport of hydrophilic high molecular weight molecular compounds such as peptides and proteins across the membrane (Bernkop-Schnürch, 2000).

However, the effectiveness of chitosan as penetration enhancer is impaired by its poor water solubility at the physiological pH. To

* Corresponding authors at: College of Marine Life Science, Ocean University of China, 5# Yushan Road, Qingdao 266003, PR China. Tel.: +86 0532 82032586; fax: +86 0532 82032586.
E-mail addresses: xjcheng@ouc.edu.cn (X.J. Cheng), jqx_1@163.com (Q.X. Ji), xgchen@ouc.edu.cn, qqsn160@163.com (X.G. Chen).

0144-8617/$ – see front matter © 2012 Elsevier Ltd. All rights reserved.
doi:10.1016/j.carbpol.2012.03.028

solve this problem, many chemical modifications of chitosan, both hydrophilic and hydrophobic, have been synthesized (Chen & Park, 2003; Li et al., 2007; Liu, Chen, & Park, 2005). Oleoyl-carboxymethyl-chitosan (OCMCS) has been proposed as one of the water-soluble chitosan derivatives over a wide pH range. We also demonstrated that OCMCS nanoparticles which had various hydrophilic polymeric chains on their surfaces were useful as drug carriers that enhanced the absorption of orally administered drugs (Sun et al., 2008).

In our previous research, oral administration of extracellular products (ECPs) of *Aeromonas hydrophila* loaded nanoparticles in carps resulted in the improved ECPs absorption (Liu et al., 2012). OCMCS nanoparticles have performed as a potent penetration enhancer of ECPs across the carp intestinal epithelium. However, we have not investigated the mechanism of OCMCS nanoparticles mucoadhesion and permeation enhancing effects for the oral delivery of hydrophilic high molecular weight drugs. In order to further explore the interaction of OCMCS particles within the physiological environment there is a need to understand how these particles behave when incubated with excised carp intestine and the polarized epithelial intestinal (Caco-2).

In the current investigation, OCMCS was synthesized with target to perform mucoadhesion and permeation enhancing effects under physiological conditions. OCMCS nanoparticles were prepared through coacervation, and FD4, a model macromolecule, was encapsulated in these nanoparticles. The physicochemical properties of nanoparticles were characterized by size, polydispersity index (PI), zeta potential and encapsulation efficiency (EE %) of FD4. The cytotoxicity of OCMCS nanoparticles was investigated in Caco-2 monolayers. The mucoadhesion of the nanosystems was evaluated using excised carp intestine. The intestinal penetration enhancement properties of nanoparticles were investigated through Caco-2 cell model and in vitro carp intestine model.

2. Materials and methods

2.1. Materials

Three different molecular weight chitosan were made from crab shell and obtained from Laizhou Haili Biological Product Co., Ltd. (Shandong China). The degree of deacetylation for the low molecular weight (LMw, 50 kDa), medium molecular weight (MMw, 170 kDa) and high molecular weight (HMw, 820 kDa) chitosan was 93.15%, 92.56%, 90.14%, respectively. Fluorescein isothiocyanate dextran (FD4), a hydrophilic and high MW molecule (Mw, 4400 Da), was purchased from Sigma Chemicals (Shanghai, China).

Caco-2 cells were obtained from the American Type Culture Collection (Rockville, MD, USA) and cultured in Dulbecco's Modified Eagle Medium (DMEM) (Gibco, Grand Island, NY, USA) containing 10% fetal calf serum. 3-(4,5-dimethylthiazol-2-yl)-2,5-diphenyltetrazolium bromide (MTT) was obtained from Amresco (Solon, OH). Common carps weighing 1500–2000 g were used for the experiments. The animal protocol was approved by Shandong Medical Laboratorial Animal Administration Committee.

2.2. Preparation of FD4-OCMCS nanoparticles

OCMCS was synthesized by reaction of chitosan with chloroactic acid and oleoyl chloride as described in our previous study (Li et al., 2006; Liu, Guan, Yang, Li, & Yao, 2001). OCMCS nanoparticles were prepared according to the mild procedure previously developed by Calvo, Remunan-Lopez, Vila-Jato, and Alonso (1997) based OCMCS polycation with TPP polyanion. The coacervation took place when the positively charged amino groups of OCMCS interacted with the negatively charged TPP. OCMCS was dissolved at 2.5 mg/ml in PBS (pH 6.5) by means of gentle stirring while FD4 was dissolved at 10 mg/ml in 1.25 ml TPP water solution obtaining the final concentration of 0.3 mg/ml. The FD4-OCMCS nanoparticles were spontaneously formed upon the incorporation of TPP to the polymer solution under vigorous stirring for 2 h. The nanoparticle suspension was stored in the dark for further use.

2.3. Characterization of FD4-OCMCS nanoparticles

The produced FD4-OCMCS dispersions were ultracentrifuged at 20,000 rpm for 30 min to separate the free FD4 in the supernatant from that loaded in the nanoparticles. The concentration of FD4 in the supernatant was determined by fluorophotometry (λ_{Ex} = 490 nm, λ_{Em} = 520 nm) using FD4-free dispersions as control experiments. The encapsulation efficiency (EE%) of FD4 was calculated as the ratio between FD4 loaded into the nanoparticles and the total amount of FD4 used for preparation of the original mixture as follows:

$$EE\% = \frac{FD4_t - FD4_f}{FD4_t} \times 100$$

where $FD4_t$ is the total amount of FD4 used for preparation of the original mixture and $FD4_f$ is the FD4 free amount recovered in the supernatant.

The sizes and size distributions of FD4-OCMCS NPs with different molecular weight were determined by Zatasier S (Malvern Instruments, Malvern, United Kingdom) at a detector angle of 90°, 670 nm, and 25.2 °C. The morphological characterizations of the FD4-OCMCS nanoparticles were viewed using scanning electron microscopy (SEM, JSM-330A, Japan) and Transmission electron microscopy (TEM, JEM-2010, Japan).

2.4. In vitro fluorescent marker release

The investigation of FD4 release from nanoparticles was performed according to Khin and Feng (2005). FD4-OCMCS nanoparticles were dispersed in transport buffer at pH 7.4, which was used to simulate physiological fluid. The solution was kept in an orbital shaker at constant gentle shaking of 110 rpm at 37 °C. Samples were removed at appropriate intervals and assayed spectrometrically at 490 nm with a UV-visible spectrophotometer (Shimadzu) to determine the release percentage of the fluorescent markers from the nanoparticles. The accumulative release percentage ($Q\%$) was calculated by Eq. (1), and the analyses were performed in triplicates.

$$Q\% = \frac{C_n \cdot V + V_i \sum_{i=0}^{n-1} C_i}{FD4_t \times EE\%} \times 100\% \quad (1)$$

where C_n is the FD4 concentration at T_n, V is the total volume of release medium, V_i is the sampling volume at T_i, C_i is the FD4 concentration at Ti (both V_0 and C_0 were equal to zero), $FD4_t$ is the total amount of FD4 used for preparation of the original mixture, *EE%* is the encapsulation efficiency of FD4 loaded into the nanoparticulate systems.

2.5. Intestinal mucoadhesion measurements

A Franz diffusion cell (Permeager, USA) with a 2 cm^2 orifice area and a donor chamber was modified as described by Bonferoni, Rossi, Ferrari, and Caramella (1999) and Rossi, Bonferoni, Ferrari, and Caramella (1999). Fresh small intestine of killed carp (1500–2000 g), was excised, rinsed with NaCl 0.9% (w/v), and cut into segments of 2 cm in length. Each segment was placed between two aluminum plates both having a 2-cm^2 slit in their centers and then placed between the donor and acceptor chambers of the cell.

The receptor chamber of the Franz cell was filled with 25 °C distilled water to keep the intestine tissue thermo-regulated. 500 μl of fluorescence-labeled nanoparticles in phosphate buffer (pH 6.5) at different concentrations (1 mg/ml, 2 mg/ml and 3 mg/ml) were placed on the excised carp intestine (area = 2 cm^2) at 25 °C and protected from light.

A 2-h incubation period was chosen to assure the attachment equilibrium. After the contact time, the nanoparticles suspension was sucked off. Samples were rinsed three times with 1 ml of distilled water for 1 min each, to eliminate nonattached nanoparticles. Subsequently, the mucous layer, including the attached nanoparticles, was scraped off the membrane and dispersed in a 5 ml solution of 1% NaOH–2% sodium dodecyl sulfate (w/v). Samples were treated for 2 h by ultrasonication and left overnight at room temperature until mucus and nanoparticles were completely dissolved. The fluorescent signal of attached nanoparticles was measured in a spectrofluorimeter with excitation and emission wavelengths of 490 and 520 nm, respectively. Results were expressed as the amount of attached nanoparticles per apparent surface (g/m^2).

2.6. Intestinal permeation measurements in vitro

The nanoparticles, suspended in Hank's Balanced Salt Solution (HBSS) buffered at pH 6.5, were subjected to permeation measurement by means of Franz diffusion cells with a 2 cm^2 orifice area (Permeagear, USA) thermostated at 25 °C (Sandri et al., 2007). The segments of carp intestine was prepared as mentioned in section 2.4, laying on a filter paper, was placed between the donor and the acceptor chambers of the Franz diffusion cell. The receptor chamber of the cell was filled with 25 °C phosphate buffer (pH 6.8). 500 μl of fluorescence-labeled nanoparticles in phosphate buffer (pH 6.5) at a concentration of 2 mg/ml were placed on the excised carp intestine at 25 °C and protected from light for 3 h.

At fixed time intervals, 500 μl samples of the acceptor phase were withdrawn and replaced with fresh buffer. FD4 was assayed by means of spectrofluorimetric detection. As control, the permeation test of FD4 solution in phosphate buffer (pH 6.5), at the same concentration of nanoparticulate systems was performed. The apparent permeability coefficient (P_{app}) was calculated using the following Eq. (2):

$$P_{app} = \frac{dQ}{dt} \cdot \frac{1}{A} \cdot C_0 \cdot 60 \quad (2)$$

where P_{app} is the apparent permeability (cm/s), dQ/dt is the permeability rate, A is the diffusion area of the membrane (cm^2), and C_0 is the initial concentration of the FD4.

2.7. Observation of nanoparticle penetration into excised carp intestine tissue by fluorescence microscope

The nanoparticle suspensions in PBS, pH 6.5, were subjected to penetration measurements in excised carp intestine tissue by means of a Franz diffusion cell. 2 h after the permeation experiments, slices perpendicular to the mucosa surface, 10 μm in thickness, were cut from the carp intestine included in the OTC Compound using a cryostat (Leica CM1510, Leica Microsystem, I) at −20 °C. The slides were observed using a fluorescence microscope (Olympus, Tokyo, Japan).

2.8. Caco-2 cell monolayer culture

Caco-2 cells, with a passage number 25–30, were cultured on polycarbonate membrane filters (pore size 0.3 μm, area 0.33 cm^2) in Corning Transwell 24-well plates (Corning Incorporated, Europe) at a seeding density of 3×10^4 cells/ml. The cells were cultured in Dulbecco's modified Eagle's medium (DMEM, Sigma, pH 7.4), supplemented with 1% (v/v) non-essential amino acids, 10% (v/v) heat-denatured fetal calf serum (FCS), 100 U/ml benzyl-penicillin and 100 U/ml streptomycin sulfate (Sigma Chemical, St. Louis, MO, USA). The culture medium was added to both the apical and the basolateral compartments and was changed every second day for 21 days. The cells were maintained at 37 °C, in an atmosphere of 95% air and 5% CO_2 at 90% relative humidity.

Afterwards, the cells were post-fixed with 1% osmium tetroxide in 0.1 M NaCac buffer (pH 7.4). The cells were then dehydrated and embedded in epoxy resin. Ultrathin sections (60 nm) were cut parallel to the coverslip, post-stained with uranyl acetate and lead citrate, and examined with a TEM FEI Tecnai 10 (Philips) at 120 kV.

2.9. Cytotoxicity test

The potential toxic effects of FD4-OCMCS nanoparticles were evaluated in vitro using Caco-2 cell lines. Caco-2 cells were seeded on 96-well plates at a density of 1×10^4 cells per well, and were cultured for 24 h. The OCMCS nanoparticle suspension (2 mg/ml) was diluted to 1000, 500, 200, 100, 50, and 20 μg/ml with culture medium, respectively. The culture medium was then replaced with the appropriate diluted nanoparticle suspension (200 μl, six replicates per sample), and the plates were incubated at 37 °C, 5% CO_2, and 95% relative humidity for 3 days. The negative control was blank culture medium.

At the end of the exposure period, MTT (20 μl) was added and incubated for an additional 4 h. Supernatants were removed, and 100 μl dimethyl sulfoxide were added. Plates were then placed on a shaking water bath at 37 °C for 10 min to dissolve the formazan salts, and the absorbances were measured at 490 nm. The percentage of viability was expressed as relative growth rate (RGR %) by Eq. (3): tests were performed in quadruplicate for each sample.

$$RGR\% = \frac{D_t}{D_{nc}} \times 100\% \quad (3)$$

where D_t and D_{nc} are the absorbances of the tested sample and the negative control.

2.10. Measurements of the transepithelial electrical resistance (TEER) and permeability studies

The transepithelial electrical resistance (TEER) across cell monolayers was monitored by means of a volt ohmmeter with a pair of chopstick electrodes (Millipore Corp. Bedford, MA, USA) during cell culture to investigate the integrity of the prepared monolayer (Sadeghi et al., 2008). Only monolayers with TEER values higher than 450 Ω cm^2 were used in the permeation study.

For the transport studies, FD4 was used in free form and in the form of nanoparticle suspensions prepared from OCMCS. Consequently, 2.0 ml of 0.25 mg/mL final concentration of FD4 and 0.25 mg/ml polymer were added to the apical side of the cell culture dish. The transport experiments were performed in HBSS at pH 6.5 (apical compartment) at 37 °C using an orbital shaker (50 rpm). The solution in the basolateral compartment was kept at pH 7.4 in all the experiments. Samples of 200 μL were withdrawn from the basolateral part at predetermined time of 15, 30, 45, 60, 120 and 240 min and replaced with equal volumes of fresh HBSS–HEPES. The samples were analyzed for the FD4 content using a fluorescence microplate reader (Polarstar, Germany). The P_{app} was calculated according to the Eq. (2).

After 2 h, the samples were carefully removed from the apical part and the cell monolayers were rinsed and replaced with fresh culture medium for evaluation of TEER recovery. The monolayers were allowed to incubate for 24 h at 37 °C in regular cell culture

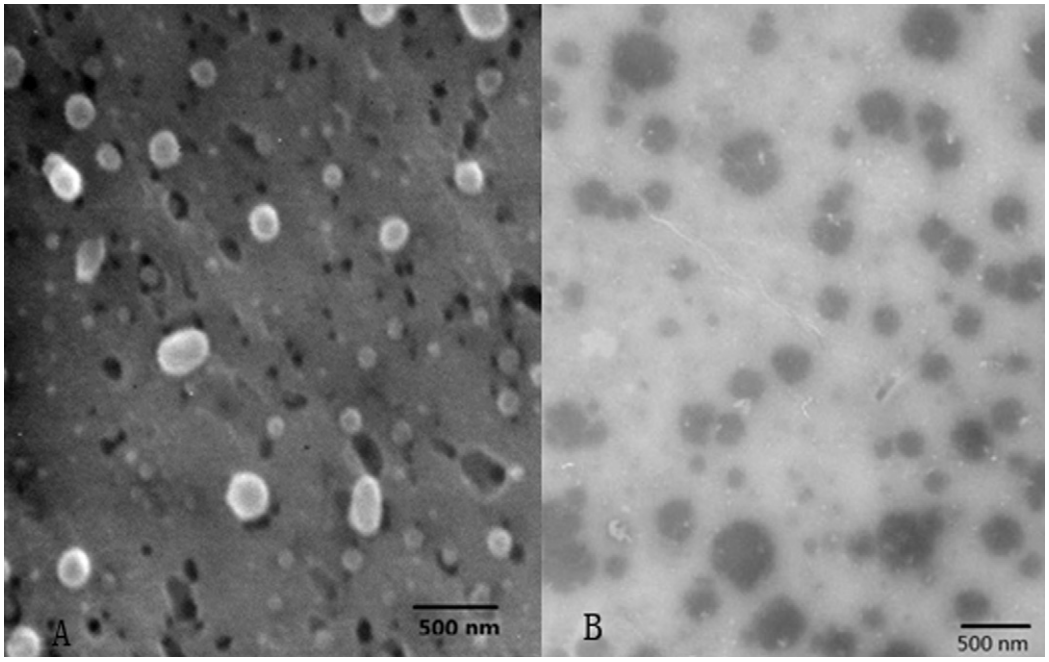

Fig. 1. Physical characterization of FD4-OCMCS II nanoparticles by SEM (A) and TEM (B) imaging.

conditions. The TEER was monitored at predetermined time intervals of 0, 0.5, 1, 2, 4, 8 and 24 h. The experiments were done in triplicate.

2.11. Statistical analysis

Statistical data analysis was performed using one way ANOVA with $p < 0.05$ as significant. All experiments were performed at least three times.

3. Results and discussion

3.1. Preparation and characterization of fluorescent NPs

The morphological characterizations of the OCMCS nanoparticles with medium molecular weight were evaluated by SEM (Fig. 1A) Fig. 1 and TEM (Fig. 1B). The nanoparticles had an almost spherical shape, similar nanometric dimension and were well dispersed without any aggregation. The encapsulation efficiency (EE) of FD4 and the particle size, zeta potential and polydispersity index (PI) of FD4-OCMCS nanoparticles measured by dynamic light scattering are presented in Table 1. FD4-OCMCS nanoparticles I, II, and III were made from FD4-OCMCS with a molecular weight of OCMCS of 50 kDa, 170 kDa and 820 kDa, respectively. FD4 was efficiently loaded into OCMCS nanoparticles I, OCMCS nanoparticles II and OCMCS nanoparticles III with an encapsulation efficiency of $78.12 \pm 9.23\%$, $76.24 \pm 6.91\%$ and $77.31 \pm 8.74\%$, respectively. Increasing the chitosan molecular weight in OCMCS nanoparticles increased the hydrodynamic mean diameter and zeta potential. All nanoparticles possessed positive surface charges of 10–20 mV. Mean diameters of the polymeric FD4-OCMCS nanoparticles I, FD4-OCMCS nanoparticles II and FD4-OCMCS III nanoparticles were around 167.41 ± 26.82 nm, 224.93 ± 40.14 and 339.24 ± 31.23 nm respectively. In the DLS measurements, the polydispersity index of all nanoparticles was below 0.25, which indicated highly monodisperse systems were obtained.

3.2. In vitro fluorescent marker release

In this study, FD4 was used as a fluorescent marker in the quantitative study of mucoadhesion and permeability measurements of nanoparticles. Fig. 2 displays the in vitro release profiles of fluorescence markers from fluorescent nanoparticles. It was found that the smaller the particle size, the faster the release from the nanoparticles. It was also found that the FD4 was released only 3.06% 4.54% and 5.35% from the FD4-OCMCS NPs (I–III) over 24 h of incubation, respectively, which was considered negligible (Zhang, Chen, Peng, & Liu, 2008).

3.3. Intestinal mucoadhesion

The amount of attached nanoparticles consisting of FD4-OCMCS with different molecular weight using the excised carp intestine as biological substrate was demonstrated in Fig. 3. The

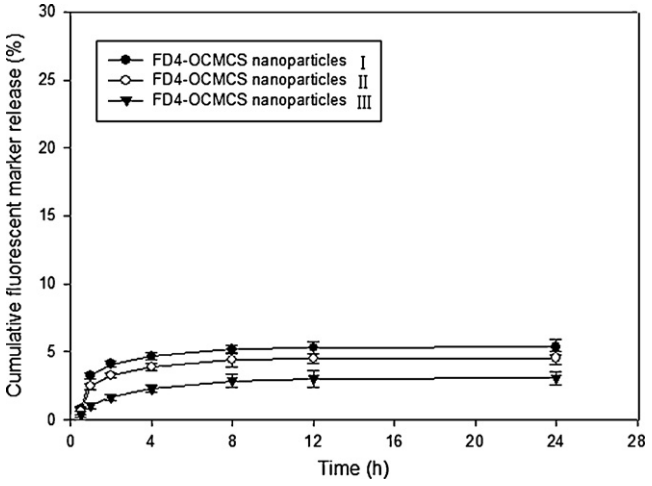

Fig. 2. In vitro cumulative percentage release of FD4 from FD4-OCMCS nanoparticles I, II, and III, respectively, incubated at 37 °C with HBSS. Data represent the mean ± SD, $n = 3$.

Table 1
Encapsulation efficiency (EE %) of FD4, mean hydrodynamic diameter, polydispersity index (PI), zeta potential, and of OCMCS NPs made by different molecular weights of chitosan.

Chitosan MW	Size (nm)	PI	Zeta potential (mV)	EE%
FD4-OCMCS nanoparticles I	167.41 ± 26.82	0.21 ± 0.02	11.54 ± 1.22	78.12 ± 9.23
FD4-OCMCS nanoparticles I	224.93 ± 40.14	0.18 ± 0.01	15.26 ± 2.32	76.24 ± 6.91
FD4-OCMCS nanoparticles III	339.24 ± 31.23	0.24 ± 0.02	19.67 ± 1.43	77.31 ± 8.74

Data represented the mean ± SD ($n = 3$).

fluorescent nanoparticles with high molecular weight presented more mucoadhesion, especially in high concentration solution. In addition, with the decrease of chitosan molecular weight, the mucoadhesion reduced in both high and low concentration solution. Although nanoparticles with lower molecular weight had smaller diameters, resulting in better adhesion tendency, the lower positive charge which might limit the occurrence of strong interactions (electrostatic and covalent) with the intestinal mucus (Bravo-Osuna, Vauthier, Farabollini, Palmieri, & Ponchel, 2007).

3.4. Intestinal permeability study in vitro

In vitro permeability studies are relevant approaches to evaluate the absorption enhancing effect of a colloidal drug carrier system on the intestinal tissue (Hillgren, Kato, & Borchardt, 1995; Watanabe, Takahashi, & Hayashi, 2004). They offer many advantages over in vivo studies: they allow more rapid determinations, require fewer animals, and generally involve simpler analytical procedures that are easier to standardize (Wadell, Bjork, & Camber, 1999). As compared to FD4 solution, all of the OCMCS nanoparticles increased the permeation of FD4 as revealed in Table 2. It was found that the apparent permeability coefficient (P_{app}) increased in correspondence to molecular weight increase from low to medium and high. The P_{app} values of FD4 in the OCMCS nanoparticulate I, IIand III were 3.61, 4.53 and 6.52 folds higher than those in the mixed solution, which were $3.85 \pm 0.57 \times 10^{-7}$ cm/s, $5.35 \pm 0.43 \times 10^{-7}$ cm/s and $7.69 \pm 0.62 \times 10^{-7}$ cm/s, respectively. The mechanism underlying the permeation-enhancing effect of chitosan seems to be based on the positive charges of the polymer, which interact with the cell membrane resulting in a structural reorganization of tight junction–associated proteins (Bernkop-Schnürch, Hornof, & Guggi, 2004; Schipper et al., 1997).

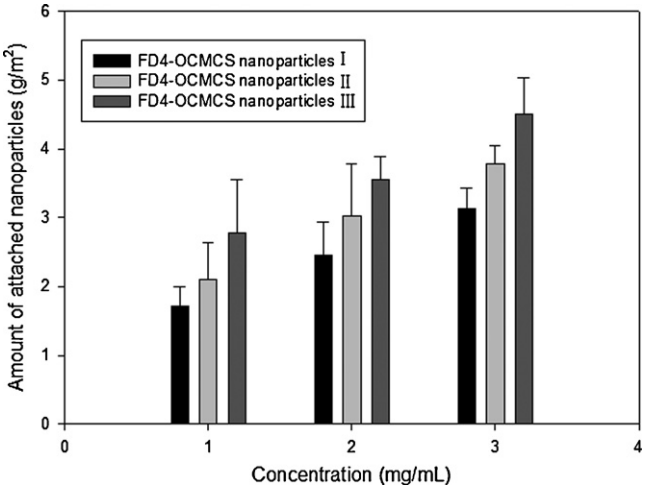

Fig. 3. Amount of attached nanoparticles consisting of different molecular weights of OCMCS.

3.5. Visualization of nanoparticle penetration into excised carp intestine tissue

The image of nanoparticles penetration into excised carp intestinal mucosa visualized by fluorescence microscope was depicted in Fig. 4. The intestinal mucosa was characterized by numerous villi whose apical part faced the intestinal lumen. After 2 h of treatment with nanoparticle samples, green fluorescent spots (that can be identified with FD4 loaded nanoparticles) could be found in the mucosal epithelia (Fig. 4A), the regions underneath the follicle associated epithelium (Fig. 4B) and the deeper regions of the secondary lymphoid organ (Fig. 4C). The results confirmed that OCMCS nanoparticles were able to interact with the intestinal tissue and be internalized in it. The nanoparticles were firstly located on the carp intestine surfaces conceivably as a consequence of the strong mucoadhesive joint between the nanoparticles and the mucus layer covering the epithelial cells (Yin et al., 2009). The mucoadhesive properties could slow down the absorption of nanoparticles into the cells with a sort of sequestering effect. In spite of this effect that could be an obstacle for nanoparticle absorption, the prolongation of the residence time offered more possibilities of nanoparticle internalization (Plapied, Vandermeulen, Vroman, Préat, & Rieux, 2010).

3.6. Cytotoxicity

Polycations are considered to be cytotoxic because cationic macromolecules could interact with cell membranes, extracellular matrix proteins and blood components leading to side effect (Kircheis, Wightman, & Wagner, 2001). The principle of MTT assay is a reduction in metabolic activity, which is an early indication of cellular damage (Hansen, Nielsen, & Berg, 1989). To test the safety of OCMCS nanoparticles as drug carriers, we evaluated the cytotoxicity to Caco-2 cells proliferation over a range of concentrations (20, 50, 100, 200, 500, 1000 μg/ml). As shown in Fig. 5, there were no significant differences between the absorbance of the negative control and the wells treated with OCMCS nanoparticles during 3 days. Thus, OCMCS nanoparticles showed no cytotoxicity and had great potential to be new drug carriers.

3.7. Evaluation of the integrity of the Caco-2 cell monolayers

The transepithelial electrical resistance (TEER) across Caco-2 monolayers was measured to evaluate the integrity of the Caco-2 cell monolayers used in the permeation experiments 21–28 days after the seeding. The initial TEER values were in the range of $664.7 \pm 63.5\ \Omega\,cm^2$ with no monolayer less than $450\ \Omega\,cm^2$, indicating integrity of the prepared monolayers, which was able to mimic the intestinal epithelium.

In order to further explore the integrity of the Caco-2 cell monolayers, the ultrathin sections were detected by TEM. The microvilli (a) and the tight junction (b) were visible in Fig. 6A.

Table 2
Apparent permeability coefficient (P_{app}) and absorption enhancement of OCMCS NPs through excised carp intestine and Caco-2 monolayer.

Nanoparticles formulation	Intestinal permeability study		Caco-2 monolayer permeability study	
	Apparent permeability coefficient ($\times 10^{-7}$ cm/s)	Absorption enhancement ratio	Apparent permeability coefficient ($\times 10^{-7}$ cm/s)	Absorption enhancement ratio
FD4 solution	1.18 ± 0.21	1	1.35 ± 0.34	1
OCMCS nanoparticles I	3.85 ± 0.57*	3.26	4.87 ± 0.39	3.61
OCMCS nanoparticles II	5.35 ± 0.43*	4.53	6.52 ± 0.67*	4.82
OCMCS nanoparticles III	7.69 ± 0.62	6.52	8.54 ± 0.59	6.32

Data represented the mean ± SD ($n = 3$).
* $p < 0.05$, there is a significant difference in P_{app} values between OCMCS nanoparticles and control group.

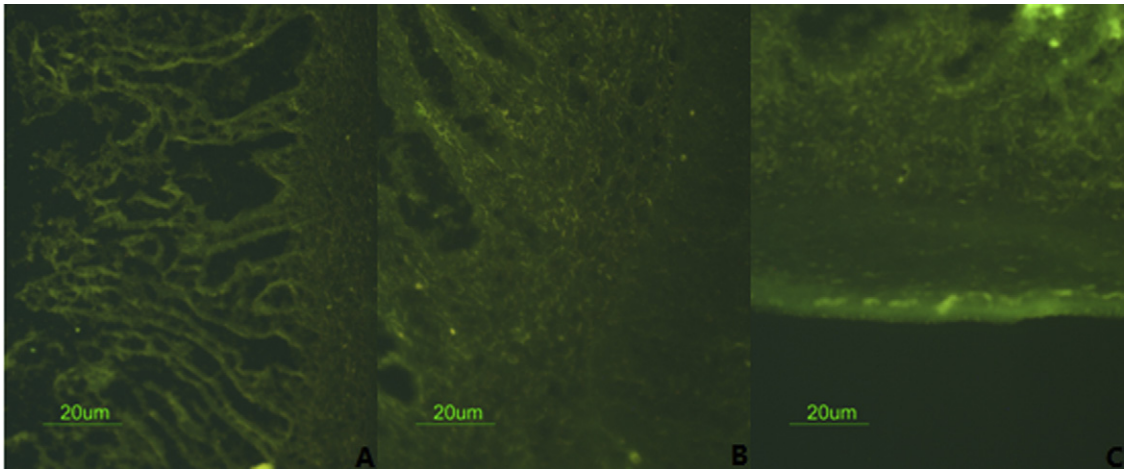

Fig. 4. Fluorescence microscopic images of carp intestine after 2 h incubation with FD4-OCMCS nanoparticles. (A) Mucosal epithelia; (B) the regions underneath the follicle-associated epithelia; (C) the deeper regions of the secondary lymphoid organ.

3.8. Caco-2 monolayer permeability experiments

The transepithelial electrical resistance (TEER) across Caco-2 monolayers was measured to evaluate the effect of the different formulations on the paracellular permeation of FD4. According to the results in Fig. 6B, the TEER values of Caco-2 monolayers incubated with FD4-OCMCS nanoparticles were significantly reduced as compared to those incubated with the FD4 solution. The effect of the FD4-OCMCS nanoparticles in opening the tight junction was immediate. A significant TEER decrease was observed within the first 30 min, after the apical addition of the FD4-OCMCS nanoparticles suspensions were added to the monolayers. The nanoparticulate system based on FD4-OCMCS I presented a slower decrease of the TEER % in comparison with all the other nanoparticles ($p < 0.05$) to indicate a slower induction of the interactions with the biological substrate. The lowering of the TEER % profiles implicates that all the nanoparticulate systems were responsible for the modulation of the cell junction integrity: this feature was also supported by the permeation of the FD4 across the cell monolayers treated with the nanoparticles (Ma & Lim, 2003; Sandri et al., 2007; Yamamoto et al., 2005a, 2005b).

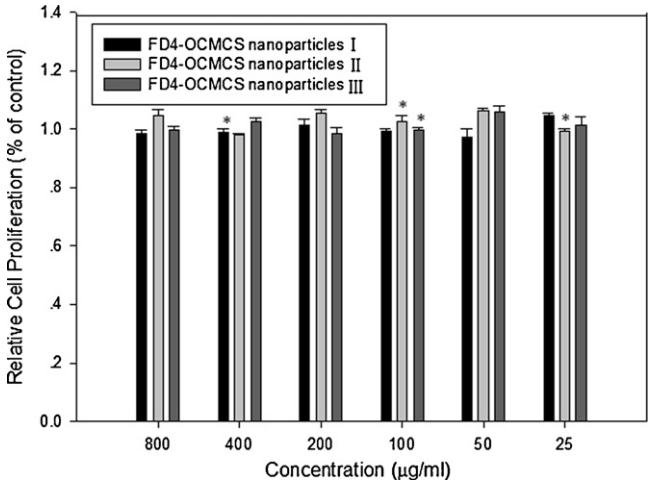

Fig. 5. In vitro cytotoxicity of FD4-OCMCS nanoparticles I, II, and III, respectively, in Caco-2 cells. Data represent the mean ± SD, $n = 6$. *$p < 0.05$ as compared with negative control.

The P_{app} (cm/s) values of FD4, which is not permeable in the presence of intact tight junctions, were calculated for all of the nanoparticulate systems as reported in Table 2. The nanoparticulate systems based on OCMCS were characterized by P_{app} values for FD4 significantly higher than that of control ($p < 0.05$). The P_{app} value of FD4 loaded in OCMCS nanoparticles I, II and III was $4.87 \pm 0.39\,cm/s \times 10^{-7}$, $6.52 \pm 0.67\,cm/s \times 10^{-7}$ and $8.54 \pm 0.59\,cm/s \times 10^{-7}$, respectively. which was significantly higher by 3.61 folds, 4.83 folds and 6.32 folds as compared to that of free FD4 ($1.35 \pm 0.34\,cm/s \times 10^{-7}$).

In addition, a good correlation was observed between the permeation enhancement properties of the different formulations and the observed reduction in TEER values during the time course of the permeation experiments. The result indicted that OCMCS nanoparticles had proved as an effective penetration enhancer of hydrophilic and/or high molecular weight molecules across the intestinal epithelium even in neutral environments by means of the mechanism (tight junctions opening and widening of paracellular pathway).

To evaluate TEER-reversibility, the monolayers were rinsed and allowed to regenerate in fresh medium after a 2 h incubation period with the different samples (Makhlof, Werle, & Tozuka, 2011). As revealed in Fig. 6B, complete recovery of the observed effects was

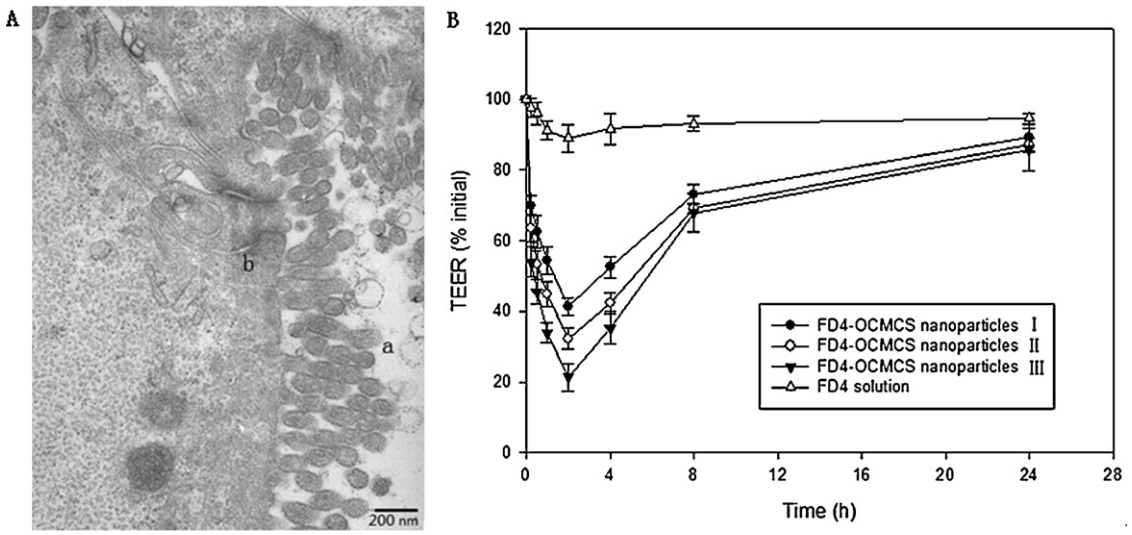

Fig. 6. (A) TEM images of flat embedded ultrathin sections of Caco-2 polarized cell monolayers (a: brush border; b: tight junction); (B) Effect of FD4 solution and FD4-OCMCS nanoparticles on the TEER values across Caco-2 cell monolayers.

achieved within 24 h, indicating that changes in permeability are not mediated through the damage of tight junctions or permanent changes of membrane function. The recovery of TEER implies that the monolayer was in its growth phase and that the observed changes in permeability were mild and reversible (Martien, Hoyer, Perera, & Schnürch, 2011).

4. Conclusions

In the present work, OCMCS was synthesized and investigated for the mucoadhesion and permeation enhancement at physiological pH. The ionotropic gelation method was suitable to prepare nanoparticles based on OCMCS with spherical morphology, uniform size, positive zeta potentials, and high encapsulation efficiency of FD4. All of the OCMCS nanoparticles with different chitosan molecular weight showed relaticely high adhesion tendency. As shown in permeation studies on Caco-2 monolayer and freshly collected carp intestinal mucosa, the OCMCS nanoparticulate system had a strong permeation-enhancing effect for FD4. The Fluorescent micrographs showed that OCMCS nanoparticles were able to adhere and infiltrate through the mucus layer, mediate to open the epithelial tight junction. Biocompatibility assessment revealed OCMCS nanoparticles were low toxicity. The preliminary results of FD4 loading and moderate mucoadhesion and permeation enhancement effect of OCMCS nanoparticles made it a suitable carrier for the oral administration of macromolecules and in particular, of peptides and soluble antisense drugs.

Acknowledgments

This work was supported by grants from the National Natural Science Foundation of China (NSFC, 81071274) and International S&T Cooperation Program of China (ISTCP, 2011DFA31270).

References

Bernkop-Schnürch, A. (2000). Chitosan and its derivatives: Potential excipients for peroral peptide delivery systems. *International Journal of Pharmaceutics*, *194*, 1–13.

Bernkop-Schnürch, A., Hornof, M., & Guggi, D. (2004). Thiolated chitosans. *European Journal of Pharmaceutics and Biopharmaceutics*, *57*, 9–17.

Bonferoni, M. C., Rossi, S., Ferrari, F., & Caramella, C. (1999). A modified cell for simultaneous assessment of drug release and washability of mucoadhesive gels. *Pharmaceutical Development and Technology*, *4*, 45–53.

Bravo-Osuna, I., Vauthier, C., Farabollini, A., Palmieri, G. F., & Ponchel, G. (2007). Mucoadhesion mechanism of chitosan and thiolated chitosan-poly (isobutyl cyanoacrylate) core-shell nanoparticles. *Biomaterials*, *28*, 2233–2243.

Calvo, P., Remunan-Lopez, C., Vila-Jato, J. L., & Alonso, M. J. (1997). Novel hydrophilic chitosan-polyethylene oxide nanoparticles as protein carriers. *Journal of Applied Polymer Science*, *63*, 125–132.

Chen, X. G., & Park, H. J. (2003). Chemical characteristics of O-carboxymethyl chitosans related to the preparation conditions. *Carbohydrate Polymers*, *53*, 355–359.

Chowdary, K. P. R., & Srinivasa Rao, Y. (2004). Mucoadhesive microspheres for controlled drug release. *Biological & Pharmaceutical Bulletin*, *27*, 1717–1724.

Dudhani, A. R., & Kosaraju, S. L. (2010). Bioadhesive chitosan nanoparticles: Preparation and characterization. *Carbohydrate Polymers*, *81*, 243–251.

Hansen, M. B., Nielsen, S. E., & Berg, K. (1989). Re-examination and further development of a precise and rapid dye method for measuring cell growth/cell kill. *Journal of Immunological Methods*, *119*, 203–210.

Hillgren, K. M., Kato, A., & Borchardt, R. T. (1995). In vitro systems for studying intestinal drug absorption. *Medicinal Research Reviews*, *15*, 83–109.

Janes, K. A., Calvo, P., & Alonso, M. J. (2001). Polysaccharide colloidal particles as delivery systems for macromolecules. *Advanced Drug Delivery Reviews*, *47*(1), 83–97.

Jinno, J., Oh, D.-M., Crison, J. R., & Amidon, G. L. (2000). Dissolution of ionizable water-insoluble drugs: The combined effect of pH and surfactant. *Journal of Pharmaceutical Sciences*, *89*, 268–274.

Khin, Y. W., & Feng, S. S. (2005). Effects of particle size and surface coating on cellular uptake of polymeric nanoparticles for oral delivery of anticancer drugs. *Biomaterials*, *26*, 2713–2722.

Kircheis, R., Wightman, L., & Wagner, E. (2001). Design and gene delivery activity of modified polyethylenimines. *Advanced Drug Delivery Reviews*, *53*, 341–358.

Li, Y. Y., Chen, X. G., Liu, C. S., Cha, D. S., Park, H. J., & Lee, C. M. (2007). Effect of the molecular mass and degree of substitution of oleoylchitosan on the structure, rheological properties and formation of nanoparticles. *Journal of Agricultural and Food Chemistry*, *55*, 4842–4847.

Li, Y. Y., Chen, X. G., Yu, L. M., Wang, S. X., Sun, G. Z., & Zhou, H. Y. (2006). Aggregation of hydrophobically modified chitosan in solution and at the air-water interface. *Journal of Applied Polymer Science*, *102*, 1968–1973.

Liu, C. G., Chen, X. G., & Park, H. J. (2005). Self-assembled nanoparticles based on linoleic-acid modified chitosan: Stability and adsorption of trypsin. *Carbohydrate Polymers*, *62*, 293–298.

Liu, X. F., Guan, Y. L., Yang, D. Z., Li, Z., & Yao, K. D. (2001). Antibacterial action of chitosan and carboxymethylated chitosan. *Journal of Applied Polymer Science*, *79*, 1324–1335.

Liu, Y., Cheng, X. J., Dang, Q. F., Ma, F. K., Chen, X. G., & Park, H. J. (2012). Preparation and evaluation of oleoyl-carboxymethy-chitosan (OCMCS) nanoparticles as oral protein carriers. *Journal of Material Science: Material in Medicine*, *23*(2), 375–384.

Ma, Z., & Lim, L.-Y. (2003). Uptake of chitosan associated insulin in Caco-2 cell monolayers: A comparison between chitosan molecules and chitosan nanoparticles. *Pharmaceutical Research*, *20*(11), 1812–1819.

Makhlof, A., Werle, M., & Tozuka, Y. (2011). Hirofumi Takeuchi. A mucoadhesive nanoparticulate system for the simultaneous delivery of macromolecules and permeation enhancers to the intestinal mucosa. *Journal of Controlled Release*, *149*, 81–88.

Mao, S., Bakowsky, U., Jintapattanakit, A., & Kissel, T. (2006). Self-assembled polyelectrolyte nanocomplexes between chitosan derivatives an insulin. *Journal of Pharmaceutical Sciences.*, *95*, 1035–1048.

Martien, R., Hoyer, H., Perera, G., & Schnürch, A. B. (2011). An oral oligonucleotide delivery system based on a thiolated polymer: Development and in vitro evaluation. *European Journal of Pharmaceutics and Biopharmaceutics*, *78*(3), 355–360.

Mohammadia, Z., Abolhassanib, M., Dorkoosha, F. A., Hosseinkhanic, S., Gilania, K., Aminid, T., et al. (2011). Preparation and evaluation of chitosan–DNA–FAP-B nanoparticles as a novel non-viral vector for gene delivery to the lung epithelial cells. *International Journal of Pharmaceutics*, *409*, 307–313.

Peppas, N. A., Bures, P., Leobandung, W., & Ichikawa, H. (2000). Hydrogels in pharmaceutical formulations. *European Journal of Pharmaceutics and Biopharmaceutics*, *50*, 27–46.

Pinto, R. C., Neufeld, R. J., Ribeiro, A. J., & Veiga, F. (2006). Nanoencapsulation II. Biomedical applications and current status of peptide and protein nanoparticulate delivery systems. *Nanomedicine: Nanotechnology, Biology and Medicine*, *2*(2), 53–65.

Plapied, L., Vandermeulen, G., Vroman, B., Préat, V., & Rieux, A. (2010). Bioadhesive nanoparticles of fungal chitosan for oral DNA delivery. *International Journal of Pharmaceutics*, *398*, 210–218.

Porporatto, C., Bianco, I. D., & Correa, S. G. (2005). Local and systemic activity of the polysaccharide chitosan at lymphoid tissues after oral administration. *Journal of Leukocyte Biology*, *78*(1), 62–69.

Rossi, S., Bonferoni, M. C., Ferrari, F., & Caramella, C. (1999). Drug release and washability of mucoadhesive gels based on sodium carboxymethylcellulose and polyacrylic acid. *Pharmaceutical Development and Technology*, *4*, 55–63.

Sadeghi, A. M. M., Dorkoosh, F. A., Avadi, M. R., Weinhold, M., Bayat, A., Delie, F., et al. (2008). Permeation enhancer effect of chitosan and chitosan derivatives: Comparison of formulations as soluble polymers and nanoparticulate systems on insulin absorption in Caco-2 cells. *European Journal of Pharmaceutics and Biopharmaceutics*, *70*, 270–278.

Sandri, G., Bonferoni, M. C., Rossi, S., Ferrari, F., Gibin, S., Zambito, Y., et al. (2007). Nanoparticles based on N-trimethylchitosan: Evaluation of absorption properties using in vitro (Caco-2 cells) and ex vivo (excised rat jejunum) models. *European Journal of Pharmaceutics and Biopharmaceutics*, *65*, 68–77.

Schipper, N. G. M., Olsson, S., Hoogstraate, J. A., deBoer, A. G., Varum, K. M., & Artursson, P. (1997). Chitosans as absorption enhancers for poorly absorbable drugs. 2: Mechanism of absorption enhancement. *Pharmaceutical Research*, *14*, 923–929.

Sun, G. Z., Chen, X. G., Li, Y. Y., Liu, C. S., Liu, C. G., Zheng, B., et al. (2008). Preparation and properties of amphiphilic chitosan derivative as a coagulation agent. *Environmental Engineering Science*, *25*(9), 1325–1332.

van der Lubben, I. M., Verhoef, J. C., van Aelst, A. C., Borchard, G., & Junginger, H. E. (2001). Chitosan microparticles for oral vaccination: Preparation, characterization and preliminary in vivo uptake studies in murine Peyer's patches. *Biomaterials*, *22*(7), 687–694.

Wadell, C., Bjork, E., & Camber, O. (1999). Nasal drug delivery—Evaluation of an in vitro model using porcine nasal mucosa. *European Journal of Pharmaceutical Sciences*, *7*, 197–206.

Watanabe, E., Takahashi, M., & Hayashi, M. (2004). A possibility to predict the absorbability of poor water-soluble drugs in humans based on the rat intestinal permeability assessed by an in vitro chamber method. *European Journal of Pharmaceutics and Biopharmaceutics*, *58*, 659–665.

Yamamoto, H., Kuno, Y., Sugimoto, S., Takeuchi, H., & Kawashima, H. (2005). Surface-modified PLGA nanosphere with chitosan improvedpulmonary delivery of calcitonin by mucoadhesion and opening of the intercellular tight junctions. *Journal of Controlled Release*, *102*, 373–381.

Yamamoto, H., Kuno, Y., Sugimoto, S., Takeuchi, H., & Kawashima, Y. (2005). Surfacemodified PLGA nanosphere with chitosan improved pulmonary delivery of calcitonin by mucoadhesion and opening of the intercellular tight junctions. *Journal of Controlled Release*, *102*(2), 373–381.

Yin, L., Ding, J. Y., He, C. B., Cui, L. M., Tang, C., & Yin, C. H. (2009). Drug permeability and mucoadhesion properties of thiolated trimethyl chitosan nanoparticles in oral insulin delivery. *Biomaterials*, *30*, 5691–5700.

Yin, Y., Chen, D., Qiao, M., Lu, Z., & Hu, H. (2006). Preparation and evaluation of lectinconjugated PLGA nanoparticles for oral delivery of thymopentin. *Journal of Controlled Release*, *116*, 337–345.

Zhang, J., Chen, X. G., Peng, W. B., & Liu, C. S. (2008). Uptake of oleoyl-chitosan nanoparticles by A549 cells. *Nanomedicine: Nanotechnology, Biology and Medicine*, *4*, 208–214.